Brain, Behavior and Evolution

Research Article

Brain Behav Evol
DOI: 10.1159/000543248

Received: September 26, 2024
Accepted: December 15, 2024
Published online: January 10, 2025

Organization of the Perioral Representation of the Primary Somatosensory Cortex in Prairie Voles (*Microtus ochrogaster*)

Carlos R. Pineda[a, b] Chris Bresee[b] Mary K.L. Baldwin[a, b] Adele M.H. Seelke[a] Leah Krubitzer[a, b]

[a]Department of Psychology, University of California, Davis, CA, USA; [b]Center for Neuroscience, University of California, Davis, CA, USA

Keywords
Cerebral cortex · Rodent · Somatosensory · Evolution · Prairie vole

Abstract
Introduction: Prairie voles (*Microtus ochrogaster*) are one of the few mammalian species that are monogamous and engage in the biparental rearing of their offspring. Biparental care impacts the quantity and quality of care the offspring receives. The increased attention by the father may translate to heightened tactile contact the offspring receives through licking and grooming. ***Methods:*** In the current study, we used electrophysiological multiunit techniques to define the organization of the perioral representation in the primary somatosensory area (S1) of prairie voles. Functional representations were related to myeloarchitectonic boundaries. ***Results:*** Our results show that most of S1 is occupied by the representation of the contralateral mystacial whiskers and the lower and upper lips. The mystacial vibrissae representation encompassed a large portion of the caudolateral S1, while the representation of the lower and upper lips occupied a large portion of the rostrolateral aspect of S1. We found that neuronal populations representing the perioral structures tended to have small receptive fields relative to other body part representations on the head and that the representation of the mystacial whiskers and perioral structures was coextensive with cytoarchitectonically defined barrel fields that extend from the caudolateral to a rostrolateral aspect of S1. ***Conclusions:*** The relative magnification of the perioral representation in S1 reflects the importance of these regions for sensory-mediated behaviors such as tactile interactions in biparental care and social bonding. This highlights how environmental and behavioral factors shape S1 organization through brain-body synergy, suggesting that relatively small changes in experience can drive adaptive cortical plasticity that, over subsequent generations, drives the cortical phenotypic diversity across the rodent clade and mammals in general.

Introduction

Prairie voles (*Microtus ochrogaster*) are small, nocturnal, and burrowing mammals native to the grass prairies and hayfields of central and eastern North America [1, 2]. Prairie voles adopt an underground lifestyle during the day and emerge at night when they navigate thick grassy undergrowth dotted by surface runways made by other ground-dwelling species [3]. Like other rodents, the prairie vole developed behavioral

Correspondence to:
Leah Krubitzer, lakrubitzer@ucdavis.edu

adaptations that involved peripheral sensory specializations and cortical organization commensurate with their nocturnal and underground lifestyle. Unlike other rodents, however, the prairie vole is one of the few socially monogamous mammalian species, forming long-lasting bonds with one individual of the opposite sex and engaging in co-parenting behaviors [4] that may significantly alter the sensory experience of the young during development.

Prairie voles experience a large amount of tactile contact shortly after birth from both parents in the form of licking and grooming, often directed at the pup's orofacial region [5, 6] (shown in Fig. 1a, b). As in other rodents, the perioral region is sensitive to tactile stimulation and subserves ethologically relevant behaviors, including parent-to-parent and parent-to-pup tactile interactions. As adults, prairie voles engage in social behaviors with their partners, including licking, allogrooming, and sniffing. Such social behaviors, specifically after mating, influence paternal behaviors shown by male prairie voles. Tactile cues from females toward their partners during gestation increase the males' propensity to engage in physical contact with infants [5]. The behaviors between parents and between parents and offspring rely, to a large extent, on the somatosensory system to support these social and parenting styles. Such behaviors are absent from long-term conspecific interactions in other nonmonogamous rodents [7]. These behavioral specializations are likely supported by the primary somatosensory cortex (S1; see Table 1 for abbreviations). In fact, natural variation in the amount of licking and grooming a prairie vole pup receives is associated with differences in cortical field size and the distribution of corticocortical connections [8, 9], indicating that tactile stimulation in developing voles has a large impact on the somatosensory system.

While the relationship between social and behavioral specializations and the organization and function of subcortical structures [10], as well as behavioral neuroendocrinology [11], have been well documented in this and other species of voles, there is relatively little known about the coevolution of these same behaviors with the organization of the sensory cortex. A previous electrophysiological recording study in our laboratory examined the organization of the sensory cortex and the gross topography of the primary somatosensory area in prairie voles [12]. However, this study did not explore the detailed organization of the perioral representations, which are critical for generating adaptive behaviors in these animals. The current study is part of a larger effort to study the neuroanatomical and functional underpinnings of social behavior in prairie voles. Here, we utilize multiunit electrophysiological recording techniques to define the detailed organization of the perioral representations in the primary somatosensory area (S1), a cortical field that processes tactile inputs that define the unique behaviors of the prairie vole.

Methods

All subjects were born and housed in the UC Davis Psychology Department vivarium. These animals were descendants of a wild stock originally caught near Champaign, Illinois. The animals were pair-housed in small laboratory cages (27 × 16 × 13 cm) in which food and water were available ad libitum. All animals were maintained on a 14:10-h light/dark cycle, with the lights on at 6:00 a.m. All experiments were performed under National Institutes of Health guidelines for the care of animals in research and were approved by the Institutional Animal Care and Use Committee of the University of California, Davis. The detailed organization of the face and perioral representations in the somatosensory cortex was examined in 9 adult prairie voles (*M. ochrogaster*) using multiunit electrophysiological recording techniques (see Table 2 for animal information). In all, 11 females and 14 males ranging in age from 5 months to 1.5 years were used in this study.

Surgical Procedures

Animals were initially anesthetized using isoflurane (2–5%) infused inside an acrylic induction chamber and then given intraperitoneal injections of 30% urethane (150 mg/kg) diluted in phosphate-buffered saline (pH = 7.4) in two doses 20 min apart, followed by subcutaneous injections of ketamine hydrochloride (30 mg/kg). Supplemental doses of urethane (150 mg/kg) or ketamine (0.5–10 mg/kg) were administered as needed for the remainder of the experiment. Respiration rate, body temperature, and pinch reflexes were monitored to ensure animals maintained a stable level of anesthesia. If supplemental ketamine was necessary to keep the animal anesthetized while supplemental doses of urethane took effect, we paused the collection of neural data until the ketamine was cleared, as indicated by the lack of spontaneous bursting activity in cortical neurons. Once anesthetized, animals were placed in a stereotaxic apparatus, and the eyes were covered with ophthalmic ointment. An incision was made along the midline of the scalp; three screws were placed on one side of the skull to provide anchor points for a head post. The craniotomy, which extended from the occipital lobe to the frontal pole, was made over the opposite hemisphere. The dura overlying

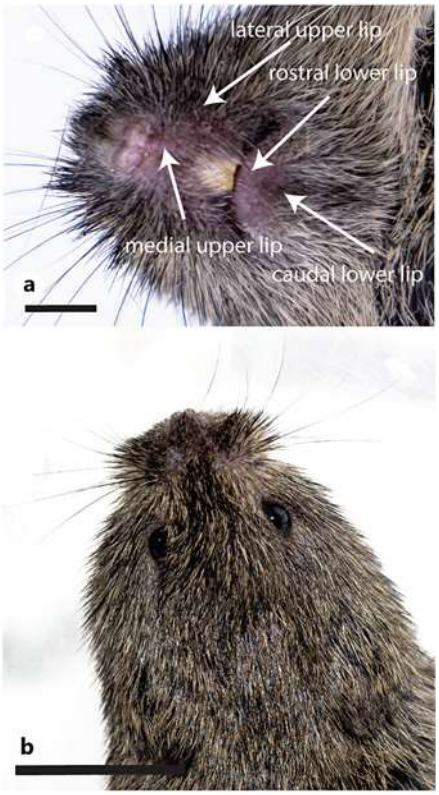

Fig. 1. Images of prairie vole morphology. **a** View of the perioral area of a prairie vole. The arrows show the division between the lateral furry upper lip and the medial upper lip, marked by a transition from thick pelage to sparsely distributed microvibrissae that line the edge of and curve into the oral cavity. The division between the macrovibrissae of the caudal lower lip and the microvibrissae of the rostral lower lip is similarly marked by a reduction in pelage close to the oral cavity. **b** Dorsal view of the head of the prairie vole. The dorsal aspect of the mystical whisker pads is visible. The scale bar in **a** represents 1 cm, and the scale bar in **b** represents 4 cm.

Table 1. List of abbreviations

Abbreviations	
ALBSF	Anterolateral barrel subfield
Aud	Auditory cortex
EN	Extranumerary barrel
FLBSF	Frontal limb barrel subfield
LJBSF	Lower jaw barrel subfield
M1	Primary motor cortex
PMBSF	Posteromedial barrel subfield
OB	Olfactory bulb
Pyr	Pyriform cortex
PV	Parietal ventral area
S1	Primary somatosensory cortex
S2	Secondary somatosensory cortex
V1	Primary visual cortex

the exposed cortex was removed, and liquid silicone was placed over the brain to prevent desiccation. Once the surgery was complete, the animals were removed from the stereotaxic frame, and the screws and skull on the contralateral hemisphere were secured to a head post with dental cement. This allowed full access to tactile stimulation of the face and body.

Multiunit Electrophysiological Recording Procedures

A digital image of the exposed cortical surface was taken using a Nikon (DSLR 5200) digital camera to relate electrode penetration sites to the surface blood vessel patterns (shown in Fig. 2a). Using a micromanipulator, an electrode was lowered to layer 4 (approximately 400 μm from the pial surface). Once the electrode was in place, tactile stimulation was manually delivered to discrete body regions using fine hand-held probes, paintbrushes, and Von Frey hairs. Extracellular population activity was recorded on-line using tungsten electrodes (FHC, Inc., Bowdoin, ME, USA) with an impedance of 3–5 MΩ. Neural activity was amplified using a head stage preamp, an amplifier with a built-in bandpass filter (low bound: 100 Hz, high bound: 5,000 Hz) (A-M Systems, Sequim, WA, USA), and sampled at 28,000 Hz with a DAQ (Power 1401 Mark II, CED, Cambridge, England). The signal was then played through a speaker and concurrently viewed as a voltage trace on a simulated oscilloscope using Spike 2 software. Signal quality (qualitative SNR) was assessed by auditory and visual inspection of the waveforms. The receptive field size and location was recorded manually on schematic images of voles. These procedures are commonly used in studies that examine the organization of S1 in a variety of mammals [12–15]. We focused on the representation of the head, face, and perioral structures but mapped portions of the representations of the forelimbs and trunk. Descriptions of the receptive fields and the type of stimulation required to elicit a response were documented, and the size, shape, and location of receptive fields were drawn on scaled illustrations of the vole body.

When the multiunit electrophysiological recording was complete, fluorescent fiducial probes (a single electrode dipped in Fluoro-Ruby: 7–10% in distilled water; KMS Medical Surgical Supplies) were inserted at strategic

Table 2. Animal information

Animal No.	Date of birth	Date of death	Age	Sex	Body weight, g	Responsive sites	Unresponsive sites	Total
18-179	July 04, 2018	October 19, 2018	195	Female	50	68	30	108
19-14	May 23, 2018	March 13, 2019	294	Male	94	60	30	90
19-41	January 05, 2018	June 17, 2019	412	Male	56	57	33	90
19-44	January 05, 2018	June 21, 2019	416	Male	63	87	29	116
19-68	May 21, 2018	July 24, 2019	429	Male	66	74	50	124
19-70	August 19, 2018	December 23, 2019	491	Male	70	54	31	85
19-72	January 09, 2018	January 17, 2020	504	Female	62	60	33	93
19-94	October 17, 2018	February 29, 2020	501	Female	54	48	28	76
19-95	March 11, 2018	March 15, 2020	498	Male	64	56	32	88
Average			415.7		64.3	62.7	32.8	95.6

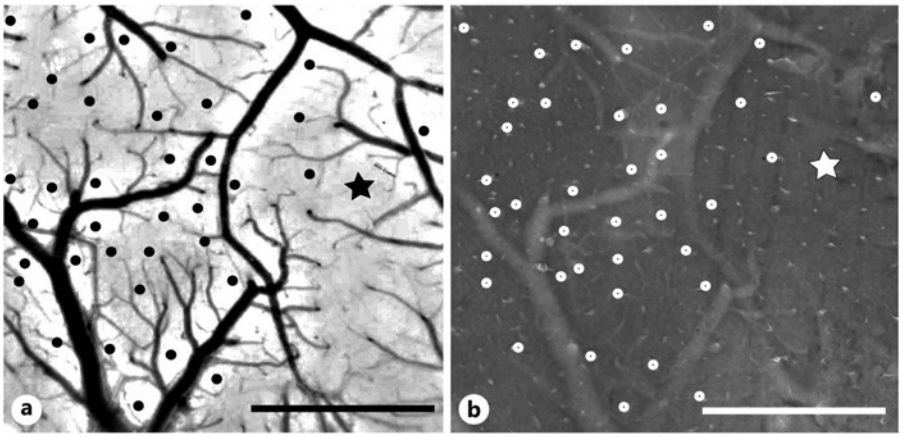

Fig. 2. Method of reconstructing electrode penetrations from multiunit electrophysiological recording experiments to histologically processed tissue in the vole neocortex. **a** Digital image of the brain surface of case 18-179 in which estimated electrode penetration locations (dark circles) were marked relative to the cortical vasculature during the experiment. **b** Superficial section of tangentially sectioned cortex stained for CO to reveal cortical vasculature. White circles denote the corresponding electrode penetration site tracts and are marked relative to cortical vasculature found on stained tissue sections. The black and white stars indicate the location of a fiducial marker (a large electrode penetration track marked with fluorescent dye), which was made during the experiment and used as part of the layer registration process. Scale bars in **a** and **b** represent 1 mm.

locations in the cortex to assist with data reconstruction (see below). Animals were then given a lethal dose of sodium pentobarbital (390 mg/kg; IP) and were perfused transcardially with phosphate-buffered saline followed by 2% paraformaldehyde in phosphate buffer (PB; pH = 7.4) and then with a 2% paraformaldehyde in PB with 10% sucrose added. The brains were then extracted from the skull, and the cortex was separated from underlying brain structures and manually flattened between glass plates. The tissue was postfixed in 4% paraformaldehyde in PB for 1 h and then transferred to a 30% sucrose PB solution for 12–48 h.

The cortex was cut into sections tangential to the pial surface on a freezing microtome. The first two superficial sections were cut at a thickness of 70 μm and processed for cytochrome oxidase (CO) to reveal the surface blood vessel patterns (shown in Fig. 2b). The subsequent sections were cut at a thickness of 30 μm and were saved in two series: one processed for CO (shown in Fig. 2b) [16] and the second processed for myelin (shown in Fig. 3)

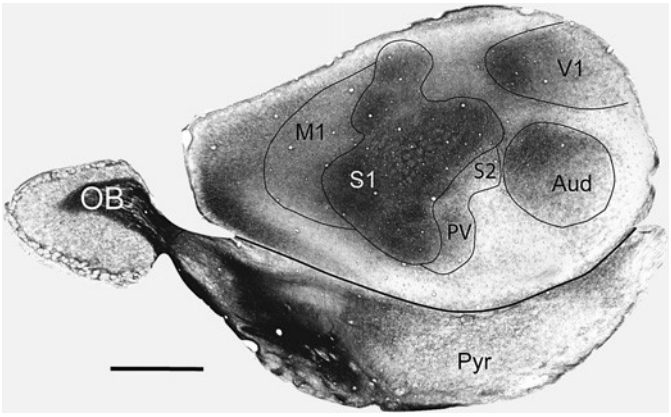

Fig. 3. Organization of the vole neocortex revealed by myelin stains. A section of flattened cortex was tangentially sectioned and stained for myelin. Primary areas S1, V1, and Aud stain darkly for myelin, and M1 stains moderately for myelin, as does S2 and PV. The entire series of myelin-stained cortical sections were used to identify the borders of sensory areas, as all borders of an area are often not seen in a single section. Solid black lines mark cortical field boundaries. The scale bar represents 3 mm. See Table 1 for abbreviations.

[17]. Once processed, sections were mounted onto glass slides and then coverslipped. Digital images were then taken of each section using an Aperio ScanScope or a Microfire camera (Optronics, Goleta, CA, USA) mounted to a Nikon E400 microscope. Images were cropped and adjusted for brightness (Adobe Inc., San Jose, CA, USA) and contrast but were otherwise unaltered.

Map Reconstructions and Measurements

Functional maps were related to anatomically defined cortical field boundaries by aligning the digital image taken before electrophysiological recording (seen in Fig. 2a) with images of processed tissue sections (seen in Fig. 2b) using Adobe Illustrator [18]. The entire series of sections were processed to reveal anatomical borders and were used to determine the extent of S1 by aligning fluorescent probes, blood vessels, and other landmarks across subsequent tissue sections. Once the physiological data were directly related to cortical architecture, Voronoi tessellations were created with an Adobe Illustrator script (https://github.com/fabianmoronzirfas/illustator-JavascriptVoronoi) based on the location of the electrode penetration sites found in images of stained tissue sections. This script creates borders at equidistant locations among adjacent electrode penetrations found on images of stained tissue sections (Fig. 2b). Voronoi Tessellations are more precise than hand-drawn interpolation lines traditionally used for constructing cortical functional maps [18, 19] and is consistent with methods previously used for measuring the relative size of representations within sensory maps [20–23]. Once maps were reconstructed, individual electrode penetrations were characterized as representing either the "face" or the "body."

Further distinctions within the face representation included the macrovibrissae of the mystacial pad, the nose, the dorsal and lateral face, and the perioral structures around the mouth. Body representations were further distinguished into neck, arm, forepaw, and forelimb representations. The hindlimb, trunk, and tail were not explored. The perioral region was divided into medial and lateral upper lip, rostral and caudal lower lip, teeth, and nose. For a complete list of the body part representations and average measurements, see online supplementary Table 1 (for all online suppl. material, see https://doi.org/10.1159/000543248). The size of the primary somatosensory cortex, the size of the cortical sheet, and the size of the barrel cortex were also measured. We restricted our measurements to those cases that showed a complete posteromedial barrel subfield (PMBSF) and anterolateral barrel subfield (ALBSF). (Measurements of S1 were calculated as a percentage of the cortical sheet, and measurements of the barrel field were calculated as a percentage of the overall size of S1 (Table 3)). Each area of the barrel field was measured separately, and the septa between each barrel structure were included. The receptive field data drawn onto scaled illustrations of multiple views of the vole body were reconstructed in Adobe Illustrator and measured using ImageJ software.

Receptive Field Measurements

Receptive fields of populations of neurons were drawn onto scaled drawings of prairie voles. These receptive field drawings were scanned and digitized in Adobe Illustrator and measured in ImageJ (Fiji) [24]. Each receptive field was then assigned to the body part parcellations divided into medial and lateral upper lip, rostral and caudal lower lip, furry buccal pad, teeth, nose, dorsal and lateral face, and macrovibrissae. Receptive field measurements can be found in Table 4.

Statistical Analysis

Voronoi tessellations allowed us to group discrete body part representations of the perioral area, such as the lower lip, upper lip, or nose, to generate maps of the perioral regions. (A full list is found in online suppl. Table 1.) It is likely that the rostrolateral extent of S1, where teeth and tongue representations have been found in other rodents [25–27], was not fully mapped, as it was difficult to access

Table 3. Architectonic measurement results

Animal No.	Cortical sheet size, mm^2	S1 area, mm^2	S1 area, % of cortical sheets	ALBSF area, mm^2	ALBSF, % of S1	PMBSF area, mm^2	PMBSF, % of S1	LJBSF area, mm^2	LJBSF, % of S1
18-179	75.52	10.01	13.25	1.43	13.51	1.47	13.92	NA	NA
19-14	65.09	15.00	23.04	1.44	9.41	2.09	13.59	0.37	2.46
19-41	67.74	15.45	22.80	1.01	7.88	1.41	11.03	0.34	2.67
19-44	68.27	13.00	19.04	NA	NA	NA	NA	NA	NA
19-68	62.68	11.74	18.73	1.20	10.53	1.40	12.26	0.44	3.91
19-70	46.60	10.96	23.51	1.62	12.42	1.96	14.98	0.52	3.98
19-72	71.36	15.97	22.38	NA	NA	NA	NA	NA	NA
19-94	47.97	13.03	27.16	1.38	12.53	1.40	12.76	0.58	5.34
19-95	47.03	11.34	24.12	NA	NA	NA	NA	NA	NA
Average	61.36	12.94	21.56	1.35	11.05	1.62	13.09	0.45	3.67
SD	11.22	2.13	4.03	0.21	2.15	0.31	1.38	0.10	1.16

Table 4. Median receptive field size per body part (in mm^2)

Body part	Median, mm^2	MAD, mm^2
Caudal lower lip	4.05	2.67
Rostral lower lip	1.75	0.71
Dorsal face	2.65	0.76
Furry buccal pad	0.37	0.02
Lateral face	11.15	1.46
Lateral upper lip	3.42	0.45
Nose	2.1	1.64
Medial upper lip	1.6	0.85
Macrovibrissae	2.22	0.98

in our experimental setup. The receptive field measurements were not normally distributed due to sample bias inherent in our experiment (we focused our population activity recording on the perioral area and head [online suppl. Fig. 1]). Thus, we calculated the median and median absolute deviation of receptive field measurements for neurons within the body part representations that compose the perioral region and for neurons in other body part representations of the head. We used a Mann-Whitney U test to quantify differences between the receptive field sizes found on different body parts. To generate average measurements across the entire subject pool, we explored the possibility of sex differences using a Mann-Whitney U test. We explored sex differences in the relative size of S1 (male = 6, female = 3) and the barrel fields (male = 6, female = 3). For all tests, $\alpha = 0.05$. Receptive field sizes between the face and the rest of the body were compared using a two-tailed t test ($n = 5$).

Results

In the following results, we first describe the histological boundaries of S1 in tissue that was sectioned tangentially and stained for myelin. We then detail the organization of the barrel fields in S1 identified using CO stains. Following this, we describe the detailed functional organization of the perioral representations, the relative amount of S1 that they occupy, and the receptive field size for neurons in different regions of the perioral representation.

Cortical Myeloarchitecture

The architectonic boundaries of different cortical fields determined using myelin stains have been previously described for voles in our laboratory [8, 12]. Briefly, here we found that the primary cortical areas, including S1, were darkly myelinated compared to surrounding fields and dominated most of the cortical sheet (shown in Fig. 3; Table 3). S1 was a large, irregularly shaped field that stained darkly for myelin compared to the moderately staining motor cortex, which was just rostral to S1. The average size of architectonically defined S1 was

12.94 mm^2 ± 2.13 (SD) and assumed 21.56% ± 4.03 (SD) of the cortical sheet. The border between S1 and cortical fields S2/PV, which are known to be adjacent to the caudolateral border of S1 in other rodent species, was readily distinguished since S2/PV stains moderately for myelin compared to S1 and the auditory cortex (shown in Fig. 3). A small strip of cortex between the caudal boundary of S1 and the rostral boundary of V1 stained lightly while V1 stained darkly for myelin. As in other rodents studied, the auditory cortex was also round and stained darkly for myelin (shown in Fig. 3).

In cortex stained for CO, cortical fields were less distinct. However, CO stains revealed well-defined barrel fields that extended from caudomedial to rostrolateral aspects of the lateral portion of S1 along with less apparent barrel zones in the rostromedial aspect of S1 (shown in Fig. 4). These architectonically defined barrel fields were coextensive with functionally defined regions of the mystical vibrissae, the perioral structures (see below) and with structures found on the forepaw, similar to that described for mice and rats [28]. Myelin and CO stains were aligned to electrode penetration sites using the location of fiducial probes and blood vessel patterns, which allowed us to confirm the location of our electrode penetrations and their relationship to cortical field boundaries and underlying barrel structures. The registration of CO and myelin-stained tissue with electrophysiologically defined perioral representations also allowed us to quantify the extent of cortex occupied by different body part representations.

The Barrel Fields

As with other rodents, prairie voles possess several barrel subfields corresponding to whiskers located on different parts of the body, primarily around the perioral area and the mystacial pad. The PMBSF and ALBSF dominated S1 and corresponded to electrophysiological representations of macro- and microvibrassae of the face and the upper jaw including the microvibrissal medial and lateral upper lip, while the lower jaw barrel subfield (LJBSF) corresponded with the representations of macro- and microvibrissae on the caudal and rostral lower lip. In several cases, the frontal limb barrel subfield (FLBSF) that represents the whiskers and paw pads of the forelimbs was visible in tissue stained for CO. However, the present study did not examine these structures in detail (shown in Fig. 4a2, b2). The PMBSF barrels of the prairie vole are organized in five rows and six columns, which corresponded with the representation of individual macrovibrissae within the mystacial pad on the face of the prairie vole. Here, we term the PMBSF by the traditional nomenclature for rats and mice; the first caudal column of straddling vibrissae was composed of four barrels identified by Greek letters δ, γ, β, and α. The remaining barrel structures in the PMBSF form a rough grid and are arranged in columns – one through five, and in five rows – A, B, C, D, and E in the medial to lateral direction. These rows and columns of barrels correspond to the rows and columns of the macrovibrissae in the mystacial pad (shown in Fig. 4d, e). In some cases, a single extranumerary whisker was observed to dorsally straddle columns 2 and 3, and this corresponded to a barrel-like structure observed in the caudal-lateral aspect of the α barrel (shown in Fig. 4d). To our knowledge, prairie voles are the only rodent to have been documented with an extranumerary barrel at this location.

Prairie voles possessed a well-defined ALBSF, which corresponded in part to the representation of the microvibrissae located on the surface of the upper lip, similar to mice and rats (shown in Fig. 4e) [29, 30]. The organization of the ALBSF relative to individual microvibrissae located in the perioral area was unclear as the arrangement of follicles for these small vibrissae was challenging to observe amidst the surrounding pelage. Unlike many rodents, the pelage between vibrissae does not become significantly thinner until very close to the mouth, making the follicle of the 45 microvibrissae difficult to localize. However, we identified some hairs as vibrissae instead of pelage due to their length, stiffness, and stereotyped shape. The LJBSF within S1 corresponded to the representations of the rostral and caudal lower lip of the prairie vole. The LJBSF, as it appeared in tissue stained for CO, was diffuse and contained irregularly shaped barrel structures (shown in Fig. 4a–c). We measured the area occupied by the ALBSF, PMBSF, and LJBSF individually to estimate the area occupied by the functional representation of the perioral structures. The PMBSF measured 1.62 mm^2 ± 0.31 (SD) and composed 13.08% ± 1.38 (SD) of S1. The ALBSF measured 1.35 mm^2 ± 0.23 (SD) and composed 11.04% ± 2.15 (SD) of S1. In comparison, the LJBSF measured 0.45 mm^2 ± 0.101 (SD) and occupied 3.67% ± 1.16 (SD) of S1. Using a Mann-Whitney U test, we found no sex differences in the overall size of the barrel cortex ($U = 11.0$, $p = 0.69$)

Topographic Organization of Perioral Structures and the Vibrissae Representation in S1

Multiunit electrophysiological population recording techniques allowed us to generate detailed maps of the perioral representations in prairie voles (shown in Fig. 5, 6; see online suppl. Fig. 2). Neurons in S1 responded to light tactile stimulation of the macrovibrissae on the

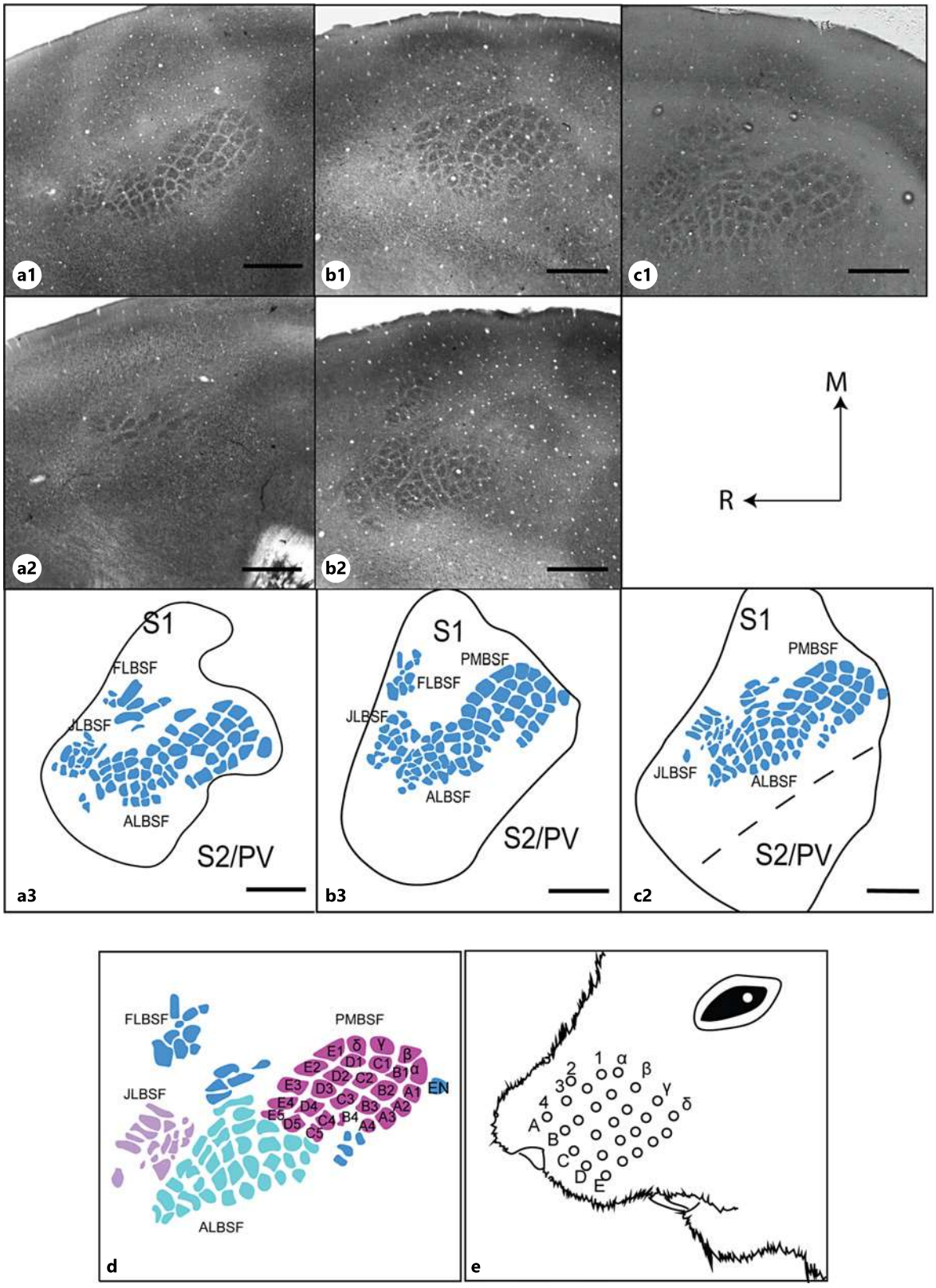

4

(For legend see next page.)

mystacial pad, the microvibrissal structures and pelage found in the lateral and medial upper lip, the macro- and microvibrissae of the lower lip, as well as the tongue, teeth, and furry buccal pad. We also found representations of the dorsal face surrounding the contralateral eye, the lateral face caudal to the mystacial pad, the ventral neck, and the proximal forelimb and forepaw. As with other rodents and mammals, the forelimbs and the neck were represented medially, while the head, face, and mouth structures were located laterally in S1 (as shown in Figs. 5c, d; 6c, d; 7a, b).

Macrovibrissae are organized in a matrix of five rows (A-E) and five columns (1–5) with an additional column of four whiskers denoted by Greek letters as previously described (shown in Fig. 4e). This functional representation of the macrovibrissae corresponded with the PMBSF barrel structures shown in Figure 4e. Not all electrode penetrations coincided with a barrel; thus, not all sites showed a principal vibrissa in the resulting receptive field. The organization of the macrovibrissae was similar across all cases (shown in Fig. 5, 6). Located just rostral to the representation of the macrovibrissae were the representation of the lateral upper lip and the medial upper lip, and the representation of the lower lip (shown in Figs. 5, 6). Microvibrissae form a continuous array encompassing the rostral extent of the macrovibrissal field to the furry buccal pad inside the oral cavity. Although it is challenging to distinguish microvibrissea from typical pelage, the microvbrissae located on the medial upper lip curve inward toward the buccal cavity, partially obscuring the upper incisors at the most roestral part of the medial upper lip (shown in Fig. 1a). The sensory representation of the microvibrissae and the sorrounding hair-bearing areas of the lower and upper lips in the primary somatosensory cortex (S1) is organized along a continuous anterior-to-posterior axis, with the midline of the rostral lower lip being represented most anteriorly in S1 and progressing toward the corner of the mouth in a caudal direction (shown in Fig. 7a, sites 1–3). The surface of the lateral upper lip extended further caudally in S1 to just below the nose (shown in Fig. 7a, sites 4–6). The nose is represented further caudal still (shown in Fig. 7a, site 7), while the tip of the snout and the dorsal aspect of the snout near the eye are at the extreme caudal position in S1 (shown in Fig. 7a, sites 8 and 9). The representation of the surface of the upper lip, including the microvibrissae, corresponded with the ALBSF, and the representation of the surface of the lower lip mapped onto the LJBSF. Representations of individual microvibrissae were impossible to identify as it was difficult to distinguish microvibrissae from the surrounding pelage (shown in Fig. 1a).

Representations of structures that compose the inside of the mouth, including the teeth, tongue, and furry buccal pad, were located laterally in S1. However, these representations were hard to access in this study due to their far lateral location in the cortex. The furry buccal pad inside of the mouth was densely covered in hairy structures. However, this area occupied a small portion of the rostral and lateral aspect of S1, lateral to the representation of the microvibrissae of the upper lip (shown in Figs. 5, 6).

Medial to the representations of the upper lip was the representation of the lower lip, which we divided into caudal and rostral surfaces. We noted the existence of large vibrissae on the furry aspect of the caudal lower lip. These vibrissae did not extend to the most rostral aspects of the rostral lower lip. Instead, the pelage became less dense, and smaller microvibrissae dominated the rostral tip of the rostral lower lip, which progressed into the oral cavity (shown in Fig. 1a). The cortical representation of the vibrissae on the lower lip was found caudal to the cortical representation of the microvibrissae on the rostral lower lip. The vibrissae situated closer to the inside of the mouth were represented in the most rostral extent of S1. The topography of the structures that compose the perioral region was similar at a gross level across cases, although there was variability in the details of these representations. The representation of the ventral neck and caudal lower lip was located medially and slightly caudally to the representation of the rostral lower lip. As with other rodents, the ventral portion of the body

Fig. 4. Organization of the orofacial region's barrel field in layer 4 of the prairie vole S1. **a1**, **a2** Digital images of the barrel field from adjacent flattened and tangentially cut tissue sections stained for CO, showing the locations of individual barrels in case 19-68. **a3** Schematic of barrels drawn from tissue stained for CO in (**a1**, **a2**). The dark line delineates the border of S1. The border of S2/PV is demarked lateral to the PMBSF. **b1**, **b2**, **c1** Digital images of barrel fields in cases 19-72 and 19-94. **b3–c2** Representative schematics of complete reconstructions showing the barrel field as in **a3**. **d** Divisions of the barrel subfields in prairie vole and classic terminology used to describe them. The colors delineate the boundaries between different barrel subfields. **e** Drawing of the lateral aspect of the prairie vole snout. The small circles represent the macrovibrissae of the mystacial pad. The row letters and column numbers indicate the identity of the whisker as it relates to the barrel cortex, denoted in other rodents. Scale bars represent 1 mm. M, medial; L, lateral. See Table 1 for abbreviations.

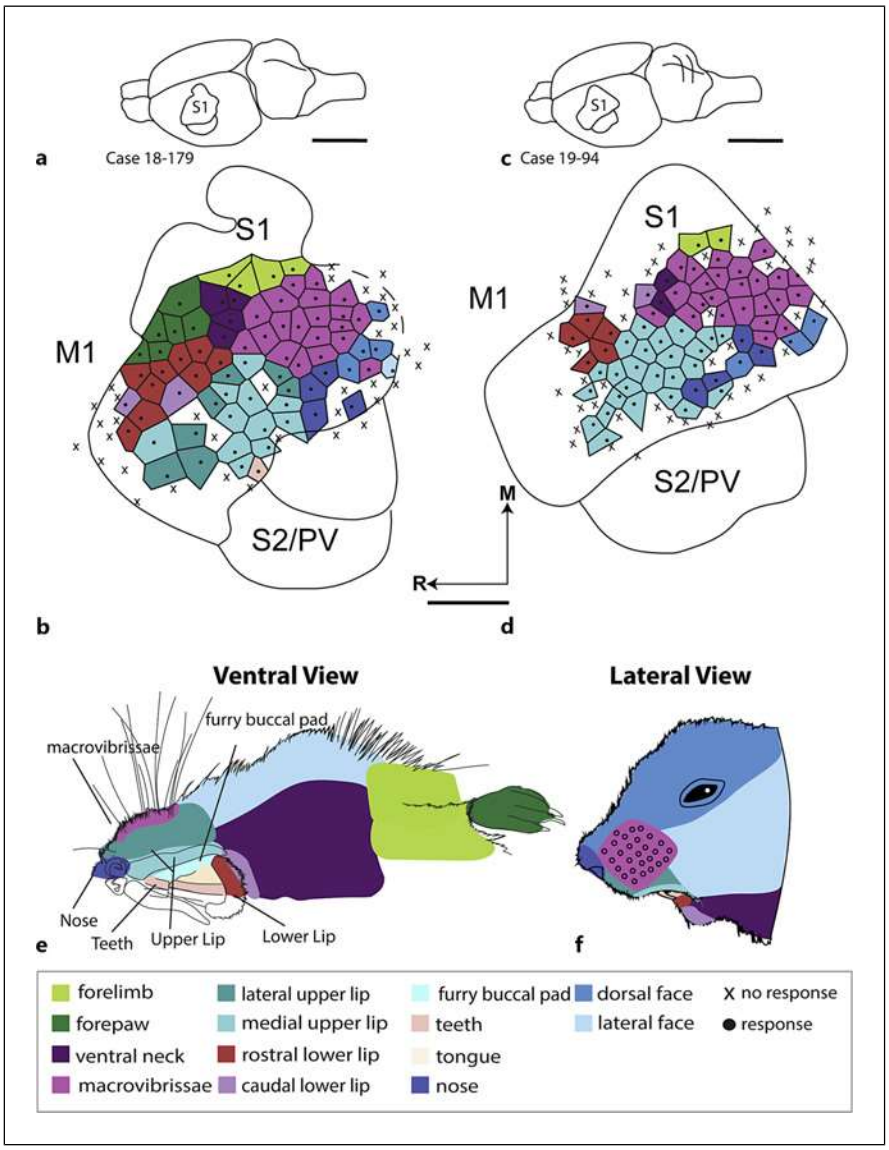

Fig. 5. Functional organization of the perioral representations in S1 in prairie voles. **a** Dorsolateral view of the brain of case 18-179 depicts the location of S1 on a dorsolateral view of the neocortex. **b** Map of the functional organization of the orofacial region produced from multiunit electrophysiological recordings. Black dots represent electrode penetration sites with Voronoi polygons drawn and colored to represent the corresponding functional body part representation revealed from tactile stimulation to the contralateral side of the body. Xs represent electrode penetration sites where neurons did not respond to tactile stimulation. The solid black lines indicate the borders of S1 identified from tissue sections stained for myelin. **c** Dorsolateral view of the brain of case 19-94 depicting the location of S1. **d** Map of the functional organization of the orofacial region as described in **b**. **e** Drawings of the ventral upper half of the prairie vole body. **f** Drawing of a lateral view of the head and face. Colors in **b** and **d** represent the major body parts of the prairie vole depicted in **e** and **f**. Bottom: key of color-coded body parts. Scale bars present in **a** and **c** represent 5 mm. Scale bars present in **b** and **d** represent 1 mm.

and head was represented rostrally, and the dorsal portions of the head and body were represented caudally. Receptive field progression within the perioral area is illustrated in Figure 7.

Receptive Field Size

We measured the size of receptive fields for groups of neurons in the perioral representations of S1 with a single electrode. Receptive field sizes were then expressed as median and MAD. We found that the smallest receptive fields were for neurons representing the furry buccal pad, the medial upper lip, and the rostral lower lip. Receptive fields on the rostral lower lip measured 1.75 mm^2 ± 0.71 (MAD) (shown in Fig. 7c), while the receptive fields on the medial and lateral upper lip measured 1.6 mm^2 ± 0.85 and 3.42 mm^2 ± 0.45, respectively (shown in Fig. 7c). Receptive fields on the caudal lower lip were larger and measured 4.05 mm^2 ± 2.67. Receptive fields of the mystacial macrovibrissae encompassed an average of 1–4 individual vibrissae surrounding a principal vibrissa and measured 2.22 mm^2 ± 0.98. These receptive fields surrounded the principal whisker but could be asymmetrical. The receptive fields on the nose measured 2.1 mm^2 ± 1.64. Curiously, the receptive fields on the dorsal face were small and measured 2.65 mm^2 ± 0.76, while the receptive fields of the lateral face were much larger, 11.15 mm^2 ±

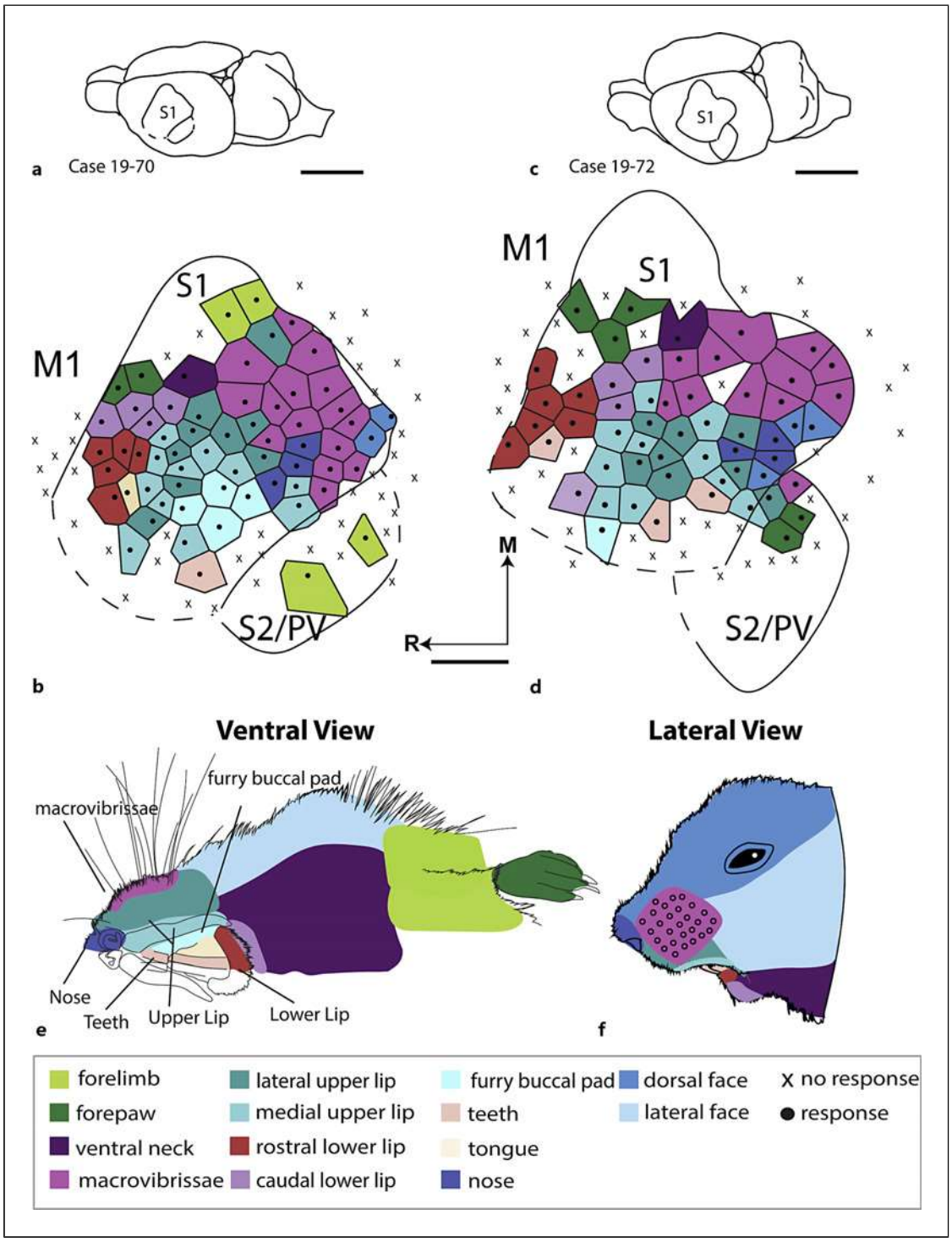

Fig. 6. Functional organization of the perioral representations in S1 in prairie voles. **a** Dorsolateral view of the brain of case 19-70 depicting the location of S1. **b** Map of the functional organization of the orofacial region produced from multiunit electrophysiological recordings. **c** Dorsolateral view of the brain of case 19-72 depicting the location of S1 within the whole brain. **d** Map of the functional organization of the orofacial region. **e**, **f** Drawings of the ventral upper half of the prairie vole body (**e**) and lateral aspect of the head and face (**f**). Conventions as in Figure 5. Scale bars present in **a** and **c** represent 5 mm. Scale bars present in **b** and **d** represent 1 mm.

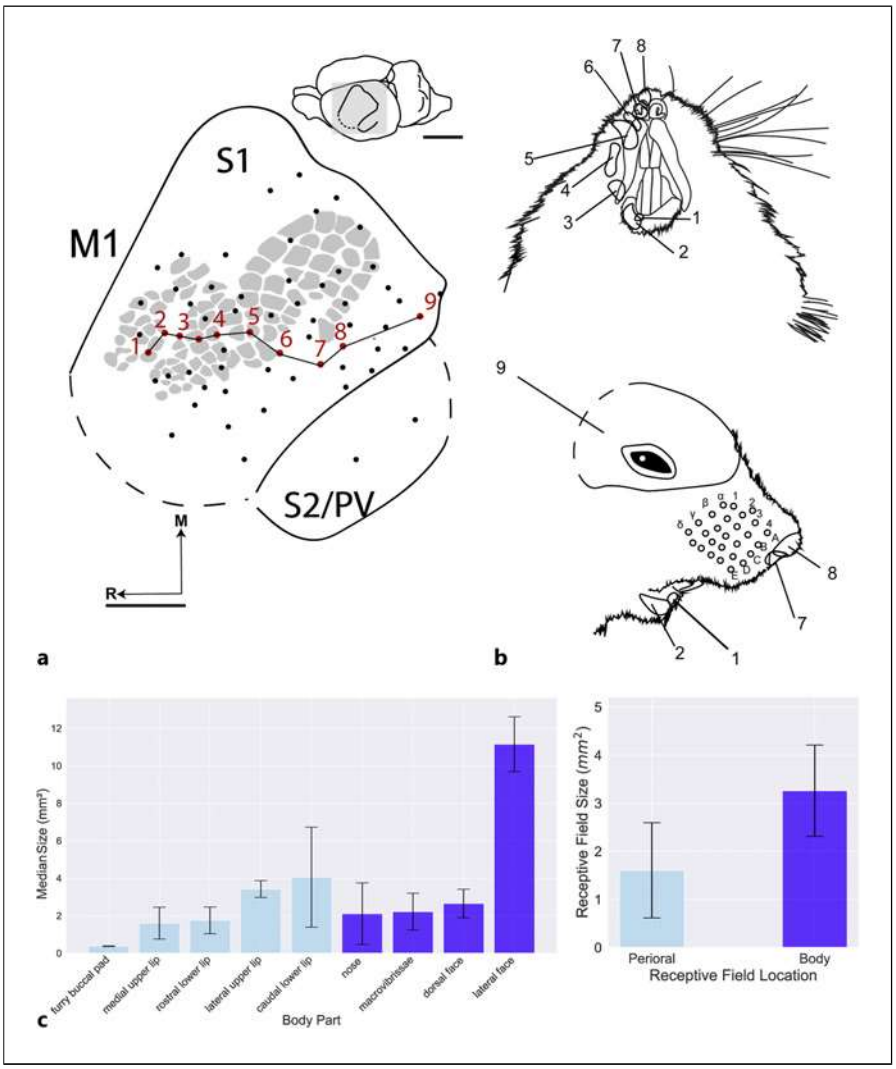

Fig. 7. Receptive field progression for neurons in the perioral face representation. **a** Illustration of S1 with a progression of electrode penetration sites from rostral to caudal (1–9). Numbers correspond with select receptive fields drawn on body parts in **b**. **b** Schematic of the vole's face, showing the locations and shapes of the receptive fields highlighted in **a**. Note that as electrode penetration sites progress from rostral to caudal, receptive fields move from ventral to dorsal surfaces of the head and face. The macrovibrissae of the mystacial pad are represented directly lateral from the forelimb (not shown), marked by the prominent PMBSF. The nose is represented lateral to the PMBSF and marked by two barrel-like structures that extend rostrally from the PMBSF (sites 7 and 8). The ventral surface of the head is represented rostrally to the macrovibrissal representation and PMBSF, with the surface of the distal lower lip represented rostral to the proximal lower lip near the oral cavity (sites 1–3). The functional representation of the lower lip is marked by the LJBSF. The surface of the upper lip is found lateral and caudal to the lower lip representation and marked by the ALBSF (sites 4–6), with the medial upper lip represented caudally (sites 5–7) and the lateral upper lip represented rostrally. **c** Bar graphs showing the median size of receptive fields of the perioral region, snout, and forelimbs in mm^2. The error bars represent the median absolute deviation. The small scale bar in **a** represents 5 mm. The large scale bar in **a** represents 1 mm. R, rostral; M, medial.

1.46. Receptive fields of the perioral region were significantly smaller than those of the rest of the face ($U = 1{,}373$, $p = 0.0005740$) (shown in Fig. 7c right), while no biological sex differences were found ($U = 3{,}615.5$ $p = 0.103$).

Discussion

In the current investigation, we utilized multiunit electrophysiological recording techniques to define in detail the functional representations of the perioral structures and vibrissae in S1 in prairie voles. As noted previously, the sensory structures on these portions of the face are associated with critical behavioral specializations in this species. We found that most of S1 is occupied by the representations of the orofacial region, particularly the macrovibrissae and upper lip, and that receptive fields for populations of neurons in these areas are small relative to other body parts. We also identified distinct histologically defined barrel fields within S1 that were coextensive with functional maps of the whiskers of the perioral region and the mystacial pad. In the following discussion, we compare the organization of the perioral representations in the prairie vole with those of other rodents, emphasizing the magnification of ethologically relevant body parts and the niche these rodents occupy.

Perioral Representations in S1 of Rodents

The cortex of the prairie vole contains a large primary somatosensory area (S1), which consists of a complete somatotopic map of the contralateral body as found in

other rodents such as rats, mice, hamsters, squirrels, naked mole rats, beavers, and capybaras, and in other mammals [31–34]. As in other mammals, the functional representation of S1 in prairie voles is inverted, with the orofacial representations located laterally and the hind limbs and tail representations located medially (see Krubitzer et al. [25] for review). The barrel cortex of the prairie vole, like that of mice, rats, and other rodent species, is divided into multiple subfields with some variation across species. These fields represent the mystical vibrissae (PMBSF) and the microvibrassae in and around the orofacial area in the upper and lower jaw (ALBSF, LJBSF). Barrel structures located medial to the LJBSF are known to represent the toe pads of the forepaw (FLBSF) and hindlimb toe pads in rats (hindlimb barrel subfield).

Early comparative work in rodents showed great variability in the organization, relative size, and appearance of the barrel structures in S1. For example, out of the 15 rodents examined by Woolsey and colleagues [35], the capybara and the beaver had no visible barrel structures in S1, while the barrels of the muskrat (another cricetid rodent) and squirrels are relatively diffuse and undifferentiated [35]. We found that much of the barrel cortex of the prairie vole is distinct and easily discernible histologically and functionally, except for the most rostral aspects of the ALBSF and LJBSF where barrels appear less structured (shown in Fig. 4). The appearance of the LJBSF in the prairie vole contrasts with that of the rat in the shape and definition as described by Pellicer-Morata and colleagues [36]. The rat possesses well-defined barrel-like structures representing vibrissae on the forelimb and hindlimb. In contrast, the prairie vole FLBSF was diffuse but present, while the hindlimb barrel subfield was not observed (shown in Fig. 4a, b) [36].

Magnification of Behaviorally Relevant Body Parts in S1 of Rodents

While previous qualitative studies indicated that prairie voles likely have a significant representation of the macrovibrissae in S1 [12], in the current study, we found that the overlapping functional and histologically defined anatomical representations of the macrovibrissae PMBSF encompassed 13.98% of S1. In contrast, the representation of the perioral area, mainly the representation of the lateral and medial aspects of the upper lip overlaying the ALBSF, encompassed 11.04% of S1 (shown in Fig. 8a). However, it should be noted that using architectonic measurements of the barrel field as a proxy for functional body representations may underestimate the extent of such representations, as electrophysiological studies show that these representations can spill outside of architectonically defined barrel fields [37].

Although scientists generally consider "rodents" as animals that rely heavily on their macrovibrissae with a magnification of the representation of these structures found in S1, this is only true for some rodents. Cortical magnification of the macrovibrissae of the mystical pad dominates S1 of rats (20% [31]) (shown in Fig. 8). In contrast, the size of the forepaw representation in the grasshopper mouse (*Onychomys leucogaster*) is relatively large (17.5%) (shown in Fig. 8) compared to that of the rat. However, the size representations of the macrovibrissae and intraoral structures appear comparatively large, though the size of S1 was not directly measured [13]. Examples of cortical magnification of the representation of body parts in other species include the buccal pad and lip surfaces in S1 of gray squirrels (19% and 32%, respectively) (shown in Fig. 8b) [33, 40], the buccal pad in capybaras (though only the representation of the head was measured) (80%) [32], and the lower lip, upper lip, and intra-oral structures in agoutis (33%) [41] (shown in Fig. 8b). Similar magnifications of the upper lip have been observed in the California ground squirrel [14]. One of the most dramatic and well-known examples of this phenomenon in rodents is the magnification of the representation of the upper and lower incisors in the naked mole rat, which occupies 31% of S1 [27]. Also of note in the naked mole rat is the enlargement of the representation of the buccal surfaces, which encompass 11.50% of S1, surround the teeth, and extend outside the buccal cavity [15, 27].

What Do Animals Do with These Morphological Specializations?

Cortical magnification of the representations of different parts of the head and body in S1 reflects their relative importance for sensory-mediated ethologically relevant behaviors [25]. This relative enlargement of the representation of a particular body part or sensory structure may reflect an increase in the number of receptors on the body and increased persistent use during the animal's lifetime [42–47]. The exact number of receptors that innervate specific body parts or how the information from those body parts is processed is poorly understood in rodents other than mice and rats. However, findings in rats and mice indicate that neurons in the orofacial whisker representation process important sensory information required to generate complex ethological behaviors such as sensory-guided locomotion, food localization, and social behaviors [15, 27], and this is likely the case in other rodents, including prairie voles.

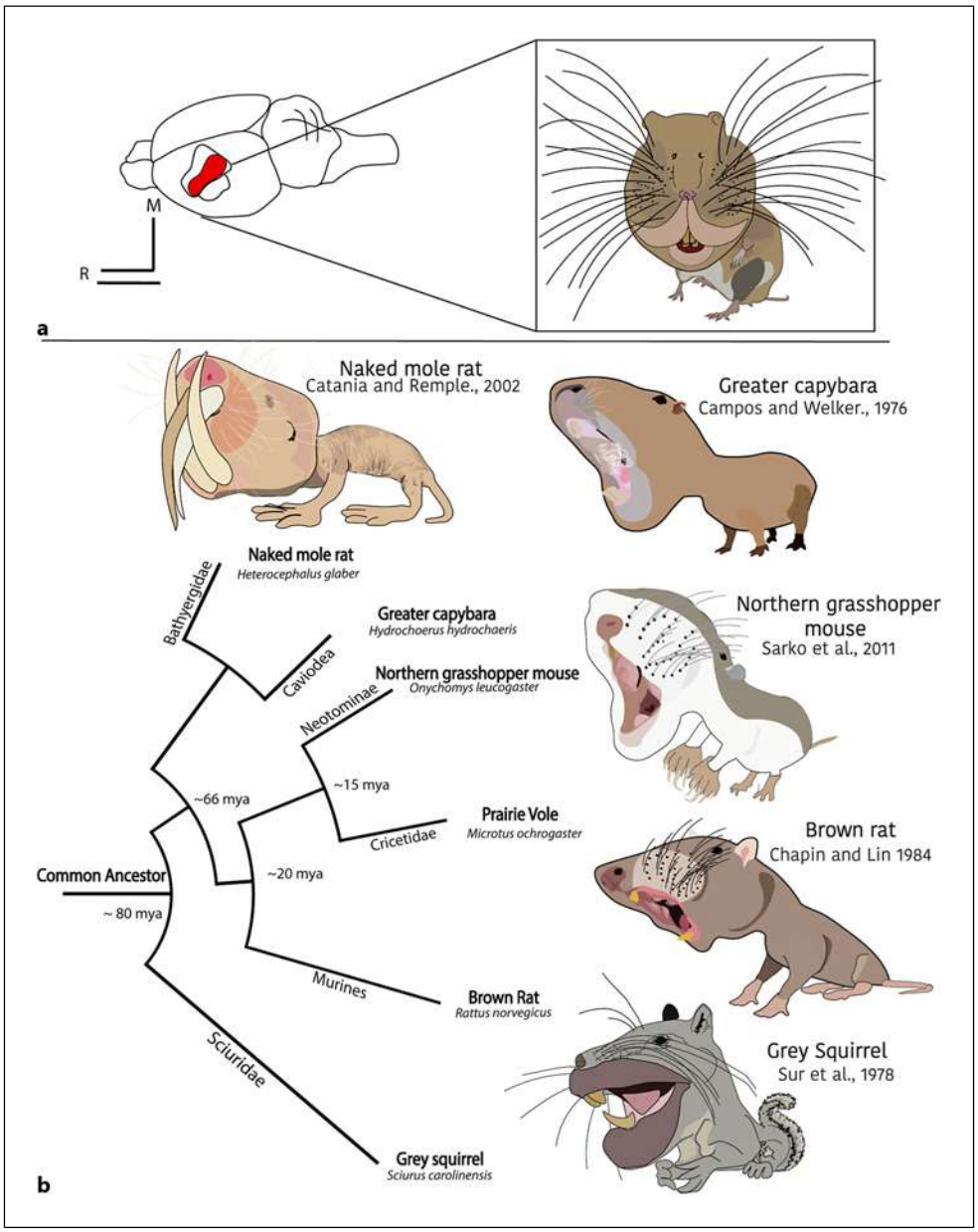

Fig. 8. Magnification of different structures of the face and body in different rodents shown schematically. **a** Drawing of the whole brain of a prairie vole (left) depicting S1, and the approximate location of the perioral representation (red inset). The "vole-unculus" (right) provides a graphical representation of cortical magnifications in the prairie vole S1. Note the expanded representation of the perioral surfaces within the primary somatosensory cortex (S1; left). **b** Phylogenetic tree of the rodent order with representative species of different families listed with accompanying graphical illustrations of cortical magnifications. While many species studied have enlarged representations of portions of the face, the magnifications are different for different species (e.g., vibrissae in rats vs. lips in squirrels). Numbers at branch nodes indicate reference time in millions of years ago [38, 39]. The scale bar in **a** represents 5 mm.

Most of what we know about the functions and relative contributions of portions of the body and head with magnified representations in S1 comes from studies of the vibrissae. For example, studies of the macrovibrissae in mice and rats show that while a single whisker can support accurate texture discrimination, discrimination of information at larger spatial scales is mediated by the macrovibrissal field as a whole [42, 48]. The macrovibrissae are not used alone during discrimination tasks but in conjunction with the microvibrissae, in which their placement upon the surface of interest is temporally correlated with macrovibrissal use [49, 50]. In addition to tactile discrimination, the whisker system in rats appears to play a substantial role in ethologically relevant behaviors. For example, neural activity in the PMBSF is highest during social interactions that involve the nose and mystacial vibrissae of rats in a gender-dependent manner [51]. The extent to which these findings may generalize to voles is a crucial question to investigate following the results described in this paper, and particularly because the vole's adaptations to monogamy and biparental care reduce the difference in gender-specific behaviors compared to other rodents.

Prairie voles and other biparental monogamous rodents, like the California mouse, appear to use their vibrissae and perioral structures for parent-to-parent and parent-to-offspring interactions, in addition to other ethological behaviors specific to their niche. For example, tactile contact between prairie vole-mated parents influences how male parents interact with their pups. Males with more direct tactile contact with their mate approached infants faster and initiated tactile contact with infants more frequently [5]. In turn, tactile experience provided by both parents to their offspring appears to affect the connectivity of the representations in S1 associated with this contact (e.g., perioral structures [8]) and influence biparental behaviors of the offspring later in life [7, 52]. Our results show that the perioral region occupies a particularly large portion of S1 in voles likely associated with these behavioral specializations.

Given what we know from studies of the vibrissal system, the cortical enlargement of different body part representations observed in rodents is likely related to the contribution of these body parts to ethologically relevant behaviors. For example, the enlarged forepaw representation of the grasshopper mouse may be the result of or support its predatory lifestyle, as it grasps fast-moving prey [13, 53]. The magnification of the incisor representation in naked mole rats is likely related to several adaptive behaviors, as behavioral observations implicate incisor use during tunnel excavation, foraging and feeding, tending to pups, and social interactions with conspecifics [54]. The relationship between cortical magnification and ethological behaviors can also be more subtle in other rodents. For example, capybaras and squirrels inhabit wide patchy habitats where food quality and quantity vary widely over seasons [55–57]. Capybaras live in seasonally flooded open savannas, are selective consumers of high-quality aquatic and nonaquatic grasses [38], and are long-term ruminators, particularly when food quality is low [39]. The enlarged representations of the lips and buccal surfaces of the capybara and ground squirrels may be part of a system that allows these animals to discriminate among food of different nutritional quality and provide sensory feedback during the manipulation of cached food in the cheek pouches.

The rodent order represents 40% of all mammals, comprising 2,277 species [25]. The common ancestor of all rodents was present 80 million years ago [58, 59], and although rodents have evolved similar overall body plans, there is remarkable diversity in their morphological specializations, behavior, and niches, which appear to be reflected in the organization of S1. Although we have discussed correlations between cortical magnification and ecological niche, the mechanisms underlying this scaling remain poorly understood. A central question is: To what extent are the differences found in the neocortex across rodents driven by progressive alterations to the developmental plan of the cortex versus alterations to the developmental plan of the body? While we formulate this question as a dichotomy, the reality is that genetically mediated morphological and cortical alterations likely happen synergistically in response to environmental context mediated by epigenetic mechanisms. This brain-body synergy is capable of remarkable plasticity, and changes in the use of a structure, like the vibrissae or perioral regions of the prairie vole, are dynamic and based on the context in which an individual develops. Variation in use, for example, in the amount of tactile contact a prairie vole pup receives can generate modifications in the cortical representation within S1 over a single lifetime, which can persist over generations if the environmental context is stable over time. However, if and how these alterations ultimately become integrated into the germ line is unknown. Recent advances in epigenetics offer clues into how persistent alterations in cortical phenotype in response to environmental factors can "tweak" developmental processes that result in stable adaptations that explain the remarkable diversity observed in the rodent clade.

Acknowledgments

We thank Cynthia Jordan for histological and surgical training and Robin Boparai for assistance in data preprocessing and analysis. We especially thank Jules Litman-Cleper for their contributions to the illustrations in Figure 8.

Statement of Ethics

All experimental protocols and animal husbandry were reviewed and approved by the UC Davis IACUC (under protocol number 19820).

Conflict of Interest Statement

The authors have no conflict of interest to declare.

Funding Sources

This research was funded by the NIH NICHHD Grant R01HD084362-01A1. These funders had no role in the design, data collection, data analysis, and reporting of this study.

Author Contributions

C.R.P. collected and analyzed the data, generated tables, illustrations, and figures, and wrote and edited the manuscript. C.B. collaborated on data collection, data analysis, and data visualization and edited the manuscript. M.K.B. collaborated on data collection and edited the manuscript. A.S. oversaw animal husbandry and edited the manuscript. L.A.K. conceived of the research, consulted on figures, and edited the manuscript.

Data Availability Statement

Data for measurements reported in the manuscript and in Figure 7 are available as supplementary tables. Photographs from which observations and illustrations were made and reported in Figures 4–7 can be made available upon request to L.A. Krubitzer and/or C.R. Pineda, as the large number of high-resolution image files is too large to host on file servers. Further inquiries can be made to L.A. Krubitzer and/or C.R. Pineda.

References

1 Armstrong DM, Armstrong DM, Choate JR, Jones JK, University TT. Distributional patterns of mammals in the plains states. Lubbock, TX. Texas Tech University Press; 1986.
2 Stalling DT. Microtus ochrogaster. Mamm Species. 1990;355:1–9. https://doi.org/10.2307/3504103
3 Oehlenschlager RJ. Notes on the prairie vole Microtus ochrogaster in Wadena county. Minnesota.
4 Kleiman DG. Monogamy in mammals. Q Rev Biol. 1977;52(1):39–69. https://doi.org/10.1086/409721
5 Simoncelli LA, Delevan CJ, Al-Naimi OAS, Bamshad M. Female tactile cues maximize paternal behavior in prairie voles. Behav Ecol Sociobiol. 2010;64(5):865–73. https://doi.org/10.1007/s00265-010-0903-6
6 Perkeybile AM, Griffin LL, Bales KL. Natural variation in early parental care correlates with social behaviors in adolescent prairie voles (Microtus ochrogaster). Front Behav Neurosci. 2013;7:21. https://doi.org/10.3389/fnbeh.2013.00021
7 Bales KL, Saltzman W. Fathering in rodents: neurobiological substrates and consequences for offspring. Horm Behav. 2016;77:249–59. https://doi.org/10.1016/j.yhbeh.2015.05.021
8 Seelke AMH, Perkeybile AM, Grunewald R, Bales KL, Krubitzer LA. Individual differences in cortical connections of somatosensory cortex are associated with parental rearing style in prairie voles (Microtus ochrogaster). J Comp Neurol. 2016;524(3):564–77. https://doi.org/10.1002/cne.23837
9 Seelke AMH, Yuan S-M, Perkeybile AM, Krubitzer LA, Bales KL. Early experiences can alter the size of cortical fields in prairie voles (Microtus ochrogaster). Environ Epigenet. 2016;2(3):dvw019. https://doi.org/10.1093/eep/dvw019
10 Young LJ, Murphy Young AZ, Hammock EAD. Anatomy and neurochemistry of the pair bond. J Comp Neurol. 2005;493(1):51–7. https://doi.org/10.1002/cne.20771
11 Bales KL, Carter CS. Developmental exposure to oxytocin facilitates partner preferences in male prairie voles (Microtus ochrogaster). Behav Neurosci. 2003;117(4):854–9. https://doi.org/10.1037/0735-7044.117.4.854
12 Campi KL, Karlen SJ, Bales KL, Krubitzer L. Organization of sensory neocortex in prairie voles (*Microtus ochrogaster*). J Comp Neurol. 2007;502(3):414–26. https://doi.org/10.1002/cne.21314
13 Sarko DK, Leitch DB, Girard I, Sikes RS, Catania KC. Organization of somatosensory cortex in the northern grasshopper mouse (Onychomys leucogaster), a predatory rodent. J Comp Neurol. 2011;519(1):64–74. https://doi.org/10.1002/cne.22504
14 Slutsky DA, Manger PR, Krubitzer L. Multiple somatosensory areas in the anterior parietal cortex of the California ground squirrel (*Spermophilus beecheyii*). J Comp Neurol. 2000;416(4):521–39. https://doi.org/10.1002/(sici)1096-9861(20000124)416:4<521::aid-cne8>3.0.co;2-#
15 Henry EC, Remple MS, O'Riain MJ, Catania KC. Organization of somatosensory cortical areas in the naked mole-rat (Heterocephalus glaber). J Comp Neurol. 2006;495(4):434–52. https://doi.org/10.1002/cne.20883
16 Wong-Riley M. Changes in the visual system of monocularly sutured or enucleated cats demonstrable with cytochrome oxidase histochemistry. Brain Res. 1979;171(1):11–28. https://doi.org/10.1016/0006-8993(79)90728-5
17 Gallyas F. Silver staining of myelin by means of physical development. Neurol Res. 1979;1(2):203–9. https://doi.org/10.1080/01616412.1979.11739553
18 Halley AC, Baldwin MKL, Cooke DF, Englund M, Krubitzer L. Distributed motor control of limb movements in rat motor and somatosensory cortex: the sensorimotor amalgam revisited. Cereb Cortex. 2020;30(12):6296–312. https://doi.org/10.1093/cercor/bhaa186
19 Halley AC, Baldwin MKL, Cooke DF, Englund M, Pineda CR, Schmid T, et al. Co-evolution of motor cortex and behavioral specializations associated with flight and echolocation in bats. Curr Biol. 2022;32(13):2935–41.e3. https://doi.org/10.1016/j.cub.2022.04.094
20 Kilgard MP, Merzenich MM. Cortical map reorganization enabled by nucleus basalis activity. Science. 1998;279(5357):1714–8. https://doi.org/10.1126/science.279.5357.1714
21 Bao S, Chan VT, Merzenich MM. Cortical remodelling induced by activity of ventral tegmental dopamine neurons. Nature. 2001;412(6842):79–83. https://doi.org/10.1038/35083586
22 Bizley JK, King AJ. Visual–auditory spatial processing in auditory cortical neurons. Brain Res. 2008;1242:24–36. https://doi.org/10.1016/j.brainres.2008.02.087
23 de Villers-Sidani E, Chang EF, Bao S, Merzenich MM. Critical Period window for spectral tuning defined in the primary auditory cortex (A1) in the rat. J Neurosci. 2007;27(1):180–9. https://doi.org/10.1523/JNEUROSCI.3227-06.2007
24 Schneider CA, Rasband WS, Eliceiri KW. NIH Image to ImageJ: 25 years of image analysis. Nat Methods. 2012;9(7):671–5. https://doi.org/10.1038/nmeth.2089
25 Krubitzer L, Campi KL, Cooke DF. All rodents are not the same: a modern synthesis of cortical organization. Brain Behav Evol. 2011;78(1):51–93. https://doi.org/10.1159/000327320
26 Remple MS, Henry EC, Catania KC. Organization of somatosensory cortex in the laboratory rat (Rattus norvegicus): evidence for two lateral areas joined at the representation of the teeth. J Comp Neurol. 2003;467(1):105–18. https://doi.org/10.1002/cne.10909
27 Catania KC, Remple MS. Somatosensory cortex dominated by the representation of teeth in the naked mole-rat brain. Proc Natl Acad Sci USA. 2002;99(8):5692–7. https://doi.org/10.1073/pnas.072097999
28 Simons DJ. Response properties of vibrissa units in rat SI somatosensory neocortex. J Neurophysiol. 1978;41(3):798–820. https://doi.org/10.1152/jn.1978.41.3.798
29 Welker C. Receptive fields of barrels in the somatosensory neocortex of the rat. J Comp Neurol. 1976;166(2):173–89. https://doi.org/10.1002/cne.901660205
30 Welker E, Van der Loos H. Quantitative correlation between barrel-field size and the sensory innervation of the whiskerpad: a comparative study in six strains of mice bred for different patterns of mystacial vibrissae. J Neurosci. 1986;6(11):3355–73. https://doi.org/10.1523/JNEUROSCI.06-11-03355.1986
31 Welker C. Microelectrode delineation of fine grain somatotopic organization of SmI cerebral neocortex in albino rat. Brain Res. 1971;26(2):259–75. https://doi.org/10.1016/s0006-8993(71)80004-5

32 Campos GB, Welker WI. Comparisons between brains of a large and a small hystricomorph rodent: capybara, Hydrochoerus and Guinea pig, Cavia;neocortical projection regions and measurements of brain subdivisions. Brain Behav Evol. 1976;13(4):243–66. https://doi.org/10.1159/000123814
33 Sur M, Nelson RJ, Kaas JH. The representation of the body surface in somatosensory area I of the grey squirrel. J Comp Neurol. 1978;179(2):425–49. https://doi.org/10.1002/cne.901790211
34 Woolsey CN. Patterns of sensory representation in the cerebral cortex. Fed Proc. 1947;6(2):437–41.
35 Woolsey TA, Welker C, Schwartz RH. Comparative anatomical studies of the SmL face cortex with special reference to the occurrence of "barrels" in layer IV. J Comp Neurol. 1975;164(1):79–94. https://doi.org/10.1002/cne.901640107
36 Pellicer-Morata V, Wang L, de Jongh Curry A, Tsao JW, Waters RS. Structural and functional organization of the lower jaw barrel subfield in rat primary somatosensory cortex. J Comp Neurol. 2021;529(8):1895–910. https://doi.org/10.1002/cne.25063
37 Brett-Green BA, Chen-Bee CH, Frostig RD. Comparing the functional representations of central and border whiskers in rat primary somatosensory cortex. J Neurosci. 2001;21(24):9944–54. https://doi.org/10.1523/JNEUROSCI.21-24-09944.2001
38 Barreto GR, Herrera EA. Foraging patterns of capybaras in a seasonally flooded savanna of Venezuela. J Trop Ecol. 1998;14(1):87–98. https://doi.org/10.1017/s0266467498000078
39 Smith CC, Follmer D. Food preferences of squirrels. Ecology. 1972;53(1):82–91. https://doi.org/10.2307/1935712
40 Krubitzer LA, Sesma MA, Kaas JH. Microelectrode maps, myeloarchitecture, and cortical connections of three somatotopically organized representations of the body surface in the parietal cortex of squirrels. J Comp Neurol. 1986;250(4):403–30. https://doi.org/10.1002/cne.902500402
41 Pimentel-Souza F, Cosenza RM, Campos GB, Johnson JI. Somatic sensory cortical regions of the agouti, Dasyprocta aguti. Brain Behav Evol. 1980;17(3):218–40. https://doi.org/10.1159/000121801
42 Diamond ME, Huang W, Ebner FF. Laminar comparison of somatosensory cortical plasticity. Science. 1994;265(5180):1885–8. https://doi.org/10.1126/science.8091215
43 Siucinska E, Kossut M. Short-lasting classical conditioning induces reversible changes of representational maps of vibrissae in mouse SI cortex--a 2DG study. Cereb Cortex. 1996;6(3):506–13. https://doi.org/10.1093/cercor/6.3.506
44 Wallace H, Fox K. Local cortical interactions determine the form of cortical plasticity. J Neurobiol. 1999;41(1):58–63. https://doi.org/10.1002/(sici)1097-4695(199910)41:1<58::aid-neu8>3.3.co;2-6
45 Seelke AMH, Dooley JC, Krubitzer LA. The emergence of somatotopic maps of the body in S1 in rats: the correspondence between functional and anatomical organization. PLoS One. 2012;7(2):e32322. https://doi.org/10.1371/journal.pone.0032322
46 Catania KC, Kaas JH. Somatosensory fovea in the star-nosed mole: behavioral use of the star in relation to innervation patterns and cortical representation. J Comp Neurol. 1997;387(2):215–33. https://doi.org/10.1002/(sici)1096-9861(19971020)387:2<215::aid-cne4>3.0.co;2-3
47 Lee KJ, Woolsey TA. A proportional relationship between peripheral innervation density and cortical neuron number in the somatosensory system of the mouse. Brain Res. 1975;99(2):349–53. https://doi.org/10.1016/0006-8993(75)90035-9
48 Celikel T, Sakmann B. Sensory integration across space and in time for decision making in the somatosensory system of rodents. Proc Natl Acad Sci USA. 2007;104(4):1395–400. https://doi.org/10.1073/pnas.0610267104
49 Brecht M, Preilowski B, Merzenich MM. Functional architecture of the mystacial vibrissae. Behav Brain Res. 1997;84(1–2):81–97. https://doi.org/10.1016/s0166-4328(97)83328-1
50 Hartmann MJ. Active sensing capabilities of the rat whisker system. Autonomous Robots. 2001;11(3):249–54. https://doi.org/10.1023/a:1012439023425
51 Bobrov E, Wolfe J, Rao RP, Brecht M. The representation of social facial touch in rat barrel cortex. Curr Biol. 2014;24(1):109–15. https://doi.org/10.1016/j.cub.2013.11.049
52 McGuire B, Novak M. The effects of cross-fostering on the development of social preferences in meadow voles (Microtus pennsylvanicus). Behav Neural Biol. 1987;47(2):167–72. https://doi.org/10.1016/s0163-1047(87)90285-8
53 Eisenberg JF, Leyhausen P. The phylogenesis of predatory behavior in mammals. Z Tierpsychol. 1972;30(1):59–93. https://doi.org/10.1111/j.1439-0310.1972.tb00844.x
54 Lacey EA, Alexander RD, Braude SH, Sherman PW, Jarvis JUM. 8. An ethogram for the naked mole-rat: nonvocal behaviors. In: Sherman PW, Jarvis JUM, Alexander RD, editors. The biology of the naked mole-rat. Princeton University Press; 2017. p. 209–42.
55 Ojasti J. Estudio biológico del chigüire o capibara. Fondo Nacional de Investigaciones Agropecuarias; 1973.
56 González-Jiménez E. Digestive physiology and feeding of the capybara. USA: CRC Press Inc; 1977. Vol. 1. p. 167–77.
57 Alho C, Rondon N. Habitats, population densities, and social structure of capybaras (Hydrochaeris Hydrochaeris, Rodentia) in the Pantanal, Brazil. Rev Bras Zool. 1987;4(2):139–49. https://doi.org/10.1590/S0101-81751987000200006
58 Steppan SJ, Schenk JJ. Muroid rodent phylogenetics: 900-species tree reveals increasing diversification rates. PLoS One. 2017;12(8):e0183070. https://doi.org/10.1371/journal.pone.0183070
59 Huchon D, Chevret P, Jordan U, Kilpatrick CW, Ranwez V, Jenkins PD, et al. Multiple molecular evidences for a living mammalian fossil. Proc Natl Acad Sci USA. 2007;104(18):7495–9. https://doi.org/10.1073/pnas.0701289104